analytical chemistry

pubs.acs.org/ac Article

Integrated Digital Microfluidics NMR Spectroscopy: A Key Step toward Automated In Vivo Metabolomics

Amy Jenne, Sebastian von der Ecken, Vincent Moxley-Paquette, Ronald Soong, Ian Swyer, Monica Bastawrous, Falko Busse, Wolfgang Bermel, Daniel Schmidig, Till Kuehn, Rainer Kuemmerle, Danijela Al Adwan-Stojilkovic, Stephan Graf, Thomas Frei, Martine Monette, Aaron R. Wheeler,* and Andre J. Simpson*

Cite This: *Anal. Chem.* 2023, 95, 5858−5866 Read Online

ACCESS | Metrics & More | Article Recommendations | Supporting Information

ABSTRACT: Toxicity testing is currently undergoing a paradigm shift from examining apical end points such as death, to monitoring sub-lethal toxicity in vivo. In vivo nuclear magnetic resonance (NMR) spectroscopy is a key platform in this endeavor. A proof-of-principle study is presented which directly interfaces NMR with digital microfluidics (DMF). DMF is a "lab on a chip" method allowing for the movement, mixing, splitting, and dispensing of μL-sized droplets. The goal is for DMF to supply oxygenated water to keep the organisms alive while NMR detects metabolomic changes. Here, both vertical and horizontal NMR coil configurations are compared. While a horizontal configuration is ideal for DMF, NMR performance was found to be sub-par and instead, a vertical-optimized single-sided stripline showed most promise. In this configuration, three organisms were monitored in vivo using ^{1}H-^{13}C 2D NMR. Without support from DMF droplet exchange, the organisms quickly showed signs of anoxic stress; however, with droplet exchange, this was completely suppressed. The results demonstrate that DMF can be used to maintain living organisms and holds potential for automated exposures in future. However, due to numerous limitations of vertically orientated DMF, along with space limitations in standard bore NMR spectrometers, we recommend future development be performed using a horizontal (MRI style) magnet which would eliminate practically all the drawbacks identified here.

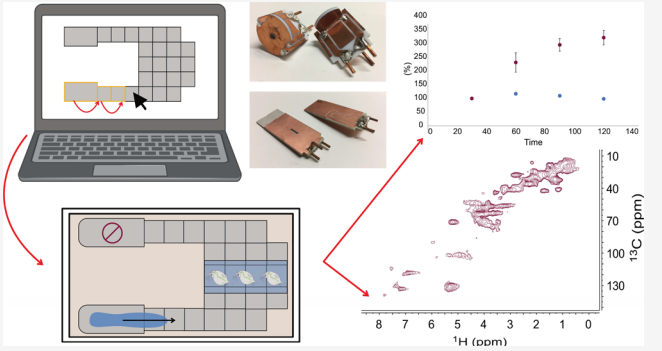

INTRODUCTION

Historically, toxicity testing has focused on apical endpoints such as reproduction and death to determine environmental thresholds.[1] However, in recent years, focus has begun shifting toward understanding the impacts of sub-lethal toxicity which requires both in vitro and in vivo methods. One important approach is the use of metabolomics, which examines changes to an organism's metabolome as a response to an external stressor.[2,3] While much progress has been made in the field,[4−7] automated in vivo methods providing information on small mass limited samples, such as small aquatic organisms and eggs, are lacking.

Nuclear magnetic resonance (NMR) spectroscopy is uniquely suited to in vivo analysis given its non-destructive nature and excellent reproducibility.[7−12] In past examples, a 5 mm flow system was used in combination with cryoprobes to dose and monitor stress response in organisms.[13−15] One such organism is *Daphnia magna*, a model species used for toxicity testing due to their prevalence in freshwater bodies and well-understood metabolome.[16] They are also key aquatic species, meaning that many food chains are dependent on their survival. *D. magna* are quite small (∼2 mm), and one of the ways they reproduce is laying resting eggs during harsh conditions (such as winter), which then hatch when ideal conditions return.[17] These eggs can be as small as ∼300 μm,[18] and the response of *D. magna* to toxins over different life stages is known to vary.[19] As such, it is important to develop NMR approaches with potential to study all life stages from egg to adult. However, while robust, NMR suffers from a lack of sensitivity which is compounded for mass limited samples.

Microcoil NMR is one possible method to address these mass sensitivity issues. Surface microcoils are particularly interesting as the sample sits directly on top, increasing mass sensitivity due to the proximity to the coil surface, and they can

Received: September 23, 2022
Accepted: March 20, 2023
Published: March 30, 2023

https://doi.org/10.1021/acs.analchem.2c04201
Anal. Chem. 2023, 95, 5858−5866

be easily redesigned to match a wide range of specific sample sizes.[18,20] Previous research has shown that matching the size of the coil to the sample size can increase sensitivity by two to three magnitudes.[21−23] In turn, the additional mass sensitivity should require fewer organisms. This is especially important as in vivo NMR monitoring requires 2D ^{1}H-^{13}C experiments to provide the additional chemical shift dispersion and in turn allow a range of metabolites to be assigned and monitored.[14] This is because magnetic susceptibility distortions from the intact organisms lead to broad lineshape in standard 1D ^{1}H NMR preventing metabolite monitoring.[24] Additionally, due to their small size, *D. magna* must be isotopically ^{13}C enriched for 2D ^{1}H-^{13}C,[25] which can become cost prohibitive for large colonies.

A further complication with using microcoils for in vivo NMR is that incorporating flow lines can be challenging. While it can certainly be done using flow-based microfluidics,[26,27] small diameter capillaries can clog, and as pumps must be situated meters away (outside the NMR magnet's field lines), back pressure from the flow system can be a potential problem such as inducing leaks and stress on the organism. Related to the above, the long capillaries represent substantial dead volumes, making it difficult to rapidly address and replace small liquid volumes over the coil. An alternative approach is the interface of digital microfluidics (DMF) and NMR.

DMF is a "lab on a chip" method decreasing sample volumes to pico- to microliters and utilizes an electric field to induce electrostatic forces on a droplet.[28,29] By activating series of electrodes, DMF allows for the dispensing, moving, mixing, and splitting of the droplets on the device.[30−33] This approach produces no pressure, and all solvents and reservoirs can theoretically be housed within the chip dimensions, reducing the need for long flow lines to the spectrometer. Additionally, as the droplet movement is software controlled, it lends itself well to automation. Work to date has demonstrated that it is possible to interface DMF to commercial NMR microcoils, while controlling the droplets from outside of the magnet,[34] which allowed chemical reactions and kinetics to be monitored.[35,36] Here, a proof-of-concept study is demonstrated which integrates custom single-sided, dual-tuned (^{1}H/^{13}C) NMR coils with in vivo sample wells, using DMF as a dosing platform. Here, the goal is to show the DMF system can be used to keep organisms alive without anoxic stress, while NMR detects their metabolome. This represents a key first step toward future automated culturing and dosing platforms for mass limited samples which have considerable potential for understanding and explaining the complex biological processes behind contaminant toxicity and synergistic effects.[37]

MATERIALS AND METHODS

DMF-NMR Device. The DMF-NMR device features three elements: (1) the vertical strip microcoil described above, which acts as the DMF top plate to complete the circuit to manipulate droplets, (2) a DMF bottom plate, and (3) a two-piece mechanical housing for each top and bottom plate. DMF bottom plates were fabricated at the University of Toronto Nanofabrication Centre (TNFC) as described elsewhere but contained 20 square DMF driving electrodes (2.25 × 2.25 mm) and two reservoir electrodes (6.6 × 16 mm).[35] The mechanical housings were 3D printed in the Wheeler Microfluidic Laboratory at the University of Toronto and explained in detail below.

Mechanical Housing. The top plate housing, the bottom plate housing, and the lock rings were designed with AutoDesk Inventor. The bottom plate housing was 3D printed in FLTOTL05 resin, and the top plate housing was 3D printed in FLHTAM01 resin using a "Form 2" 3D printer (Formlabs). Post-printing, the housings were washed two times in isopropanol for 10 min to remove any un-crosslinked resin, dried with pressurized air to clear all the inner channels, and then cured under UV light for 2 h at 80 °C. The lock rings were 3D printed in PLA (filament.ca.) using an "Ultimaker 2" 3D printer (ultimaker.com).

DMF Device Assembly and Operation. DMF bottom plates were fixed in the housing with Scotch Brand single-sided tape (3 M). Microcoil top plates were fixed in the housing with Scotch Brand insulation tape (3 M). Bottom plates were joined to top plates by spacers formed from two (or three) layers of Scotch Brand double-sided tape (3 M), approximately 200 μm (300 μm, respectively) thick as previous work has illustrated.[35,36] Additionally, two layers of Scotch Brand single-sided tape (3 M) were wrapped around the top plate housing and the bottom plate to reinforce the system, and then wrapped with Teflon tape (local hardware store) to slow evaporation. All the tape used was far enough from the coil region to not contribute NMR signal. The lock rings, which were designed to fit the specific geometry of the gradient and cover of the TXI probe to hold the DMF chip and coil secure while in the magnet, were placed on top of the gradient and the cover attached to the probe. These rings allow the assembled DMF-NMR device to be inserted into the probe and locked in place by turning the upper lock-ring by 20−70°. The DMF devices' bottom plates were interfaced through the printed circuit board (PCB) pogo-pin interface to a DropBot digital microfluidic control system running MicroDrop software, which is described in detail elsewhere.[34] The PCB pogo-pin interface design was formed in KiCAD (www.kicad-pcb.org) as previously described.[35] The PCBs were fabricated by PCBway (Shenzhen JDB Technology Co., Ltd.). The ground-electrode of the microcoil top plate was connected to the probe internally,[35] where the DropBot "ground" was grounded externally from the probe. Droplets were actuated by applying sine waves of up to 155 VRMS at 8 kHz between the top-plate electrode and successive electrodes on the bottom plate, either manually or in pre-programmed sequences for automation.

***Daphnia magna* Culturing.** Organisms were originally purchased from Ward's Scientific, but cultures have been maintained in house since 2017. *D. magna* cultures undergo a 40% media change three times per week and are fed simultaneously. Organisms are cultured in a 16:8 light/dark cycle and at a density of 1 daphnid/10 mL. Organisms used for this experiment were fed ^{13}C *Chlamydomonas rheinhardtii* (purchased from Silantes GmbH) from birth until ∼2 weeks old. Cultures were at least two generations old (born from ^{13}C enriched parents), thus considered 99% isotopically enriched.[25] Prior to experimentation, organisms were switched to natural abundance algae, grown in house, to clear the gut and ensure that NMR signals are exclusively from the organism. Once the gut is cleared, organisms are ready for in vivo NMR experiments, with their media/food placed as droplets on the DMF device (and in the sample well) to provide oxygen to the organisms during experimentation, and ensure that stress responses were not from starvation. The food added was enough to sustain the organisms but below the detection limits of the NMR as previously reported.[7]

https://doi.org/10.1021/acs.analchem.2c04201
Anal. Chem. 2023, 95, 5858−5866

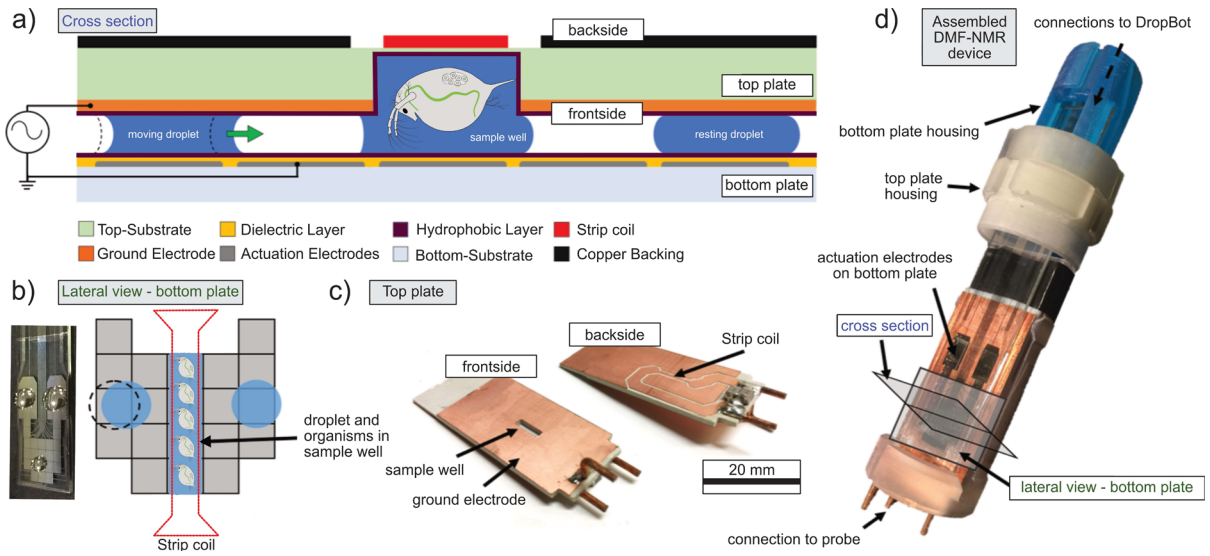

Figure 1. DMF-NMR overview. (a) Schematic radial cross-section of the DMF-NMR device. DMF bottom plate, and strip coil with sample well acting as the DMF top plate (ground electrode), *D. magna* in the sample well, and additional media droplets. (b) Schematic lateral view of the DMF-NMR device along with a photo of the DMF chip. (c) Photos of both sides of the optimized microcoil. (d) Fully assembled DMF-NMR device with an image of the DMF chip, electrical connection (as in previous work)[35,41] to external control electronics not shown.

In Vivo Stress Response Experiments. Depending on the experiment, three or five *D. magna* were placed inside the sample well in the microcoil immediately prior to placement in the NMR with two droplets of 4 μL each placed onto the DMF device containing organism media and food. The DMF-NMR system was assembled as described above, inserted into the NMR probe, and then fed through the NMR, with cables connected to the DropBot. Droplets are held in place using the DMF interface, until ready to move. NMR experiments were started immediately, and new droplets were brought into the system every 30 min. As a proof-of-concept to determine whether the DMF-NMR system could sustain organisms, a simple stress response was measured. In the control experiments, droplets were brought into the system as described to maintain organism health. In the exposure tests, no droplets were brought in to examine stress responses due to the switch to anerobic respiration. Experiments were complete after 2 h, to ensure organism survival, and completed in triplicate.

NMR Experiments. Experiments were conducted on a Bruker Avance 500 MHz NMR using a Bruker modified TXI probe.[38] ^{1}H-^{13}C HMQCs (phase sensitive using echo/antiecho gradient selection with decoupling) were collected using an adiabatic shape pulse (Crp60, 0.5, 20.1, 500 μs), 2048-time domain points, 64 increments, a relaxation delay of 0.25 s, 64 scans (in vivo experiments), 1536 scans (ex vivo experiment), and 4 scans (microcoil comparison experiments). The version of HMQC used here was chosen as it was previously found to be optimal (amongst a wide range of HSQC and HMQC variants tested) for 2D NMR on double-tuned single-sided planar coils with inhomogeneous B_1 profiles,[39] and the 90° pulse was calculated for each experiment. For coil comparison experiments, samples of ^{13}C-D-glucose (500 mM) described above were used to compare the signal to noise ratio (SNR), line shape, and nutation curves to determine the best signal response.

Spectral Assignments. Metabolite identification was performed using AMIX (Analysis of MIXtures software package, version 3.9.15, Bruker BioSpin, in combination with the Bruker Bio-reference NMR databases version 2-0-0 through 2-0-5). Spectra were calibrated using tyrosine and D-glucose resonances using the Bruker Bio-reference NMR databases. Assignments were performed using a procedure previously described.[40] Relative changes in metabolites during in vivo exposure were found using MestReNova 14.1.0 using spectral stacks and the peaks graphs resulting from global spectral deconvolution, plotted as relative percent changes.

For further information regarding the reagents, samples, and microcoil design and fabrication, please see the Supporting Information.

RESULTS AND DISCUSSION

Overview of DMF-NMR. To better understand the results, it is important to have a clear visualization of the combined DMF-NMR system. Figure 1 outlines all the components fabricated and used in this study to keep *D. magna* alive in the assembled system. Following this overview, a discussion of the fabricated microcoil used, the maximum metabolomic response on the microcoil, and an anerobic stress response using the combined system will be discussed.

Optimizing Coils for DMF-In Vivo Experiments. DMF functions by using an electric field which induces electrostatic forces on a droplet, allowing movement as the voltage moves across electrodes. Traditionally, DMF systems operate in a horizontal orientation. However, in previous work, DMF-NMR interfaces have been developed with a vertical orientation[35,36] due to space constraints inside the NMR and a lack of planar horizontal NMR microcoils to act as a top plate. While vertical orientations work, higher voltages are required to move the droplets via DMF, and continuous actuation (a constant voltage to keep the droplets from falling with gravity) is required to maintain droplet location and integrity. Minimizing this voltage increases the longevity of the device; thus, when considering an ideal DMF-NMR interface, it is useful to investigate the feasibility of horizontal integration.

Unfortunately, while a horizontal orientation is better for DMF, it is currently not ideal for NMR spectroscopy in a vertical-oriented narrow bore magnet. This is due to lack of space in the horizontal plane, vertical-oriented shim stacks

https://doi.org/10.1021/acs.analchem.2c04201
Anal. Chem. 2023, 95, 5858−5866

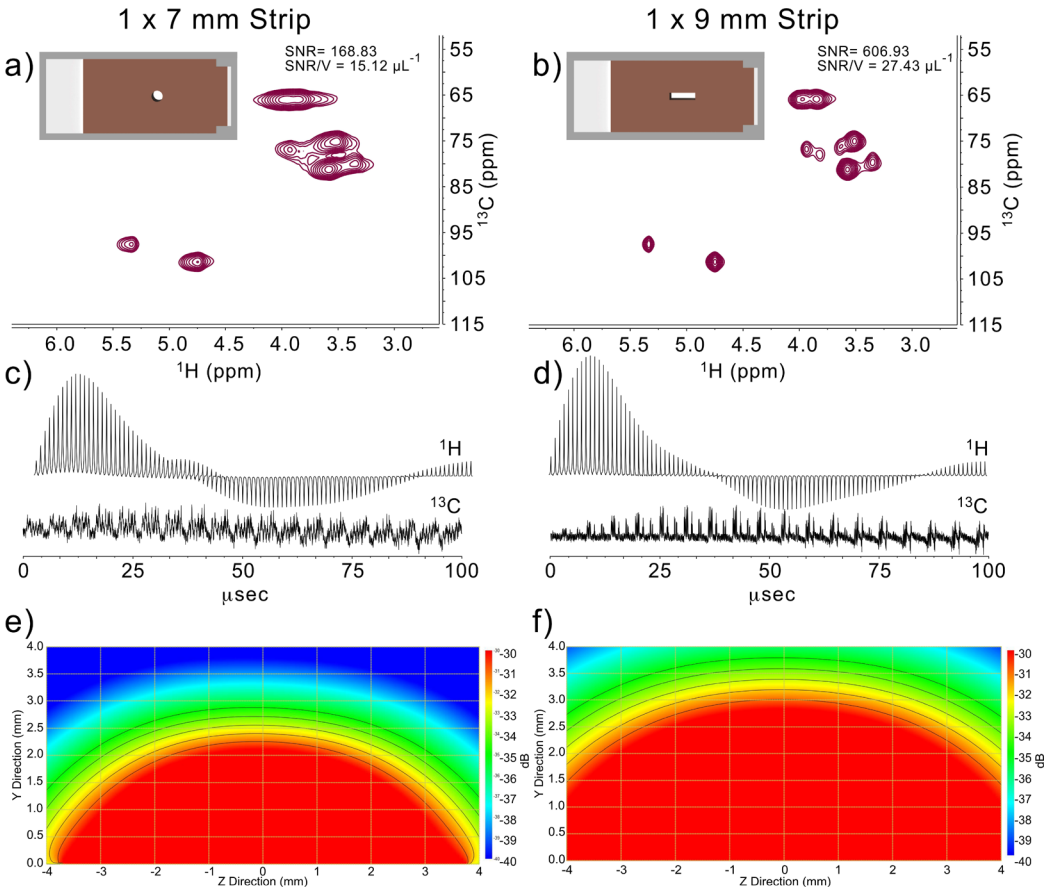

Figure 2. Comparison of two vertical stripline coils. (a,b) 2D HMQC of ^{13}C-D-glucose with the measured SNR and a diagram of the coil setup, (a) 1 × 7 mm strip coil, and (b) 1 × 9 mm strip coil, respectively. Note, the coils are not pictured, so the sample well can be seen clearly. The coils are strips that run over the entire sample well. (c,d) ^{1}H and ^{13}C nutation curves of each coil on D-sucrose and ^{13}C-D-glucose, respectively. (e,f) Feko simulations of the magnetic flux density from −30 to −40 dB.

(optimized for long vertical samples, not flat horizontal ones), and a general lack of microcoils that generate in-plane B_1 fields. Specifically, in a standard vertical NMR, the applied magnetic field (B_o) is vertical (Z), so a standard NMR coil creates a B_1 field orthogonal to this (X,Y) to "flip" the spins for detection. However, if a planar coil is already oriented horizontally to create a field along X,Y, it must generate a field that runs across its surface rather than perpendicular to it. Practically, all NMR microcoils designed to date are aligned vertically and generate perpendicular B_1 fields.[18,21,38,42−47] As such, before a horizontal DMF system can be considered, it must be determined whether a horizontal planar coil can be designed with acceptable lineshape, sensitivity, and penetration depth. Ultimately, the questions become "how compromised is the NMR performance of horizontal coils when compared to vertical orientations?" as well as "are these losses acceptable for in vivo DMF-research?"

To investigate this, five microcoils were created that can be utilized with DMF inside a modified NMR probe. Three were horizontal and shaped as a strip,[22,42] spiral,[48,49] and butterfly,[50] (see Figure S1), each with a 3 mm round sample well. For comparison, the other two were vertically oriented strip coils with differing sample wells (see Figure 2). The results of the horizontal coils are discussed in the Supporting Information.

To test the performance of vertical orientations, striplines were chosen as they have been shown previously to produce the best lineshape and sensitivity combination.[38,48] The two vertical strip coils were created with different sample wells. The first strip was a 1 × 7 mm microstrip (to match those previously published)[38] with the same sample well as the horizontal coils (fits up to three *D. magna*) to permit direct comparison to the horizontal designs. The second coil is a more optimized 1 × 9 mm microstrip with a longer sample well (fits up to five *D. magna*) more compatible with the NMR's Z-oriented shim stack.

Figure 2 compares the two vertical coils. The first strip with an identical sample well to the horizontal configuration (Figure S1) shows a SNR of 168, over three times more than the best performing (butterfly) horizontal coil along with improved lineshape. The nutation curve is not ideal but is vastly improved over the horizontal strip (Figure S1d−f). In a vertical orientation, it is also possible to extend the length of the strip (and sample well) increasing the space for organisms as well as improving the vertical aspect ratio of the design to allow optimal shimming. This is not feasible in the horizontal position as samples are tough to shim given the limited XY shims (compared to comprehensive Z shims) on a standard vertical NMR system. Here, the second vertical coil was designed with a longer strip, and as a result, the signal to noise per unit volume (SNR/V) doubles, along with a drastic improvement in lineshape, becoming less than what is commonly seen in living organisms (<50 Hz). The nutation curve is far from ideal when compared to a volume coil but is consistent with that expected from a single-sided design,[42] and

https://doi.org/10.1021/acs.analchem.2c04201
Anal. Chem. 2023, 95, 5858−5866

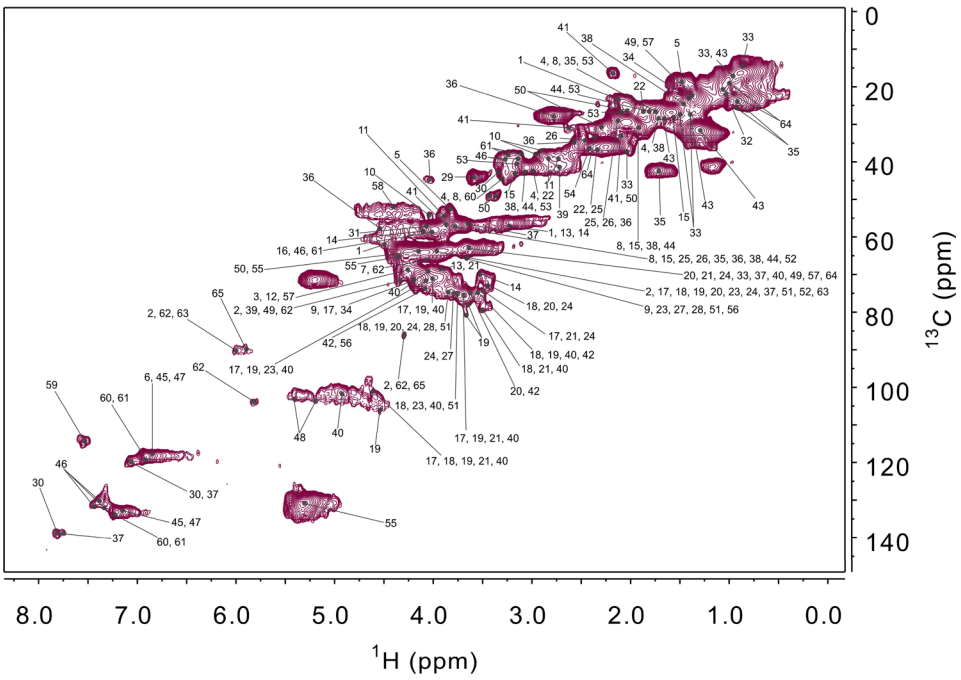

Figure 3. 2D ^{1}H-^{13}C HMQC of five ex vivo *D. magna* on the dual-tuned (^{1}H/^{13}C) vertical strip coil. See Table S1 for metabolite identities.

both ^{1}H and ^{13}C show enough inversion to allow high-quality HMQC data to be collected. When the absolute SNR from the large sample well is considered (~606.9), it is roughly 10 times that seen for the best horizontal configuration. Arguably, this is an approximate comparison of the "optimal" horizontal and vertical configurations and is valid given that larger samples can be shimmed vertically. As such, when the lack of space and poor lineshape are considered, it becomes hard to justify a horizontal DMF configuration in a narrow bore vertical NMR system. Moving forward, the best performing vertical microcoil will be used for the combination with DMF.

Evaluating Metabolomic Response. Prior to interfacing DMF-NMR to maintain the organisms in vivo, it is important to ensure enough signal can be collected to allow metabolic discrimination and assignment using the optimal (1 × 9 mm strip) vertical coil. To obtain maximum signal, the sample well was filled with five *D. magna*. Organisms were alive when added to the coil but died during the 12 h experiment. Figure 3 shows the HMQC data, which contains a wide range of metabolites, impressive seeing as only ~1 mg of dry weight (~0.2 mg per organism) is present. In previous in vivo work examining *D. magna* (20 organisms) using a 5 mm flow system and a cryoprobe, the maximum number of metabolites found in both an 8 and 24 h experiment was 67. Here, in a 12 h experiment, the maximum number of metabolites found was 65. Their identities can be found in the Supporting Information. Results here indicate that the microcoils provide a comparable response in terms of metabolite monitoring potential. The additional mass sensitivity in this study from the microcoils partially balances the gains from the cryocooling and greater biomass in the previous work.[14] Here, to improve sensitivity, only 64-increments were used in the HMQC with the additional time saved used for additional scans. While it is possible to use non-uniform sampling (NUS)[51] and while 50% sampling is normally sufficient for complex environmental samples,[52] when tested here, we found artifacts due to the reduced number of increments. Ultimately, given the unknown nature of the real signals and potential for artifacts, we decided against its use. If in the future experiments can be run with more increments, then NUS requires further investigation. However, the results are encouraging and indicate that the vertical microcoil setup holds potential for in vivo studies if organisms can be kept alive inside the small sample well.

In Vivo Exposure Using a DMF System. With a single-sided dual-tuned strip coil, integration with DMF is possible. In this new integration, the DMF chip and printed electrodes were designed to work in tandem with the optimized microcoil (the coil acting as the ground plate). The entire system is connected to a computer program outside of the magnet, allowing for full automation of the droplets.[34] Once completed, the system can be used to re-supply water, food, and nutrients to the organisms or in the future even expose the organisms to contaminants under automation. Previously, DMF-NMR has been utilized for reaction monitoring, kinetics, and biomolecular sensing,[35,36,53] but this is the first attempt to sustain organisms in vivo inside an NMR. Furthermore, while DMF cell culturing is relatively common,[54] we are aware of only a single previous report that describes the use of DMF to culture multi-cellular organisms.[55] To accomplish DMF culturing of *D. magna*, as a proof-of-concept, the DMF-NMR setup was used to examine anerobic stress in *D. magna*. In each experiment, three *D. magna* were placed in the sample well with ~20 μL of water, resulting in ~0.6 mg of biomass, with two additional droplets of *D. magna* media (containing oxygen and algae) 4 μL each held in place on the DMF chip away from the sample well.

In one set of experiments, the DMF system was used to bring these droplets to the organisms every 30 min and these were defined as the control organisms. In the other set of experiments, the system was set-up the same way as in the control organisms, but no additional droplets are brought to the organisms in the sample well. In this set of experiments, the *D. magna* use up the oxygen quickly as there is only ~20 μL in the sample well, after which point, they begin to undergo an

https://doi.org/10.1021/acs.analchem.2c04201
Anal. Chem. 2023, 95, 5858−5866

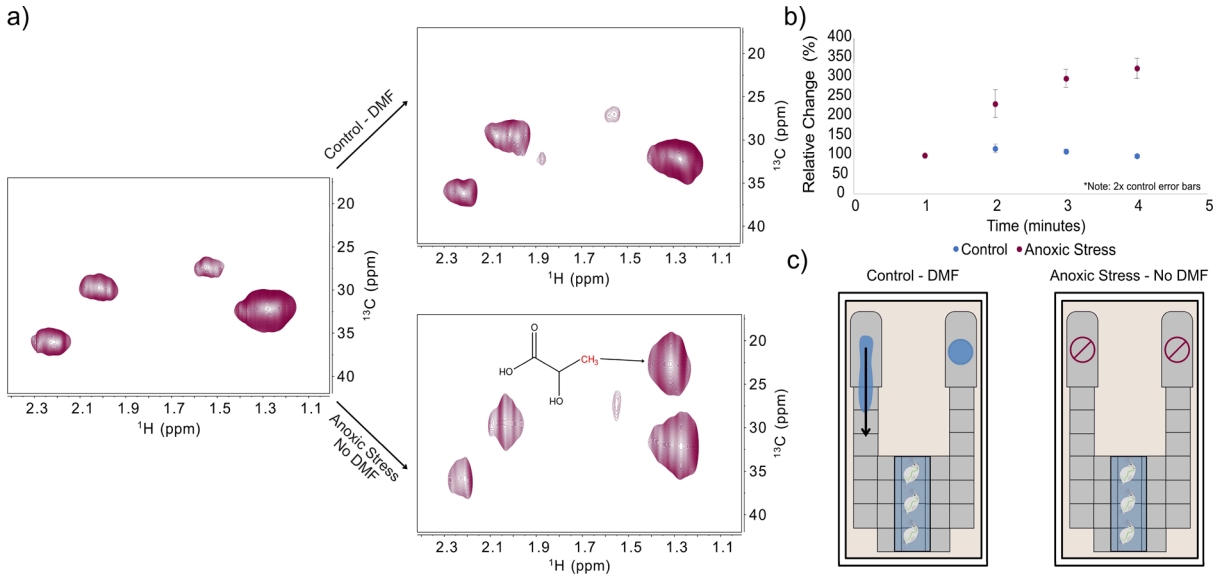

Figure 4. Workflow of the interfaced DMF-NMR system as a proof-of-concept automated exposure platform. (a) 2D of the aliphatics of the *D. magna* inside the microcoil where lactic acid would occur. In the control, droplets were used to maintain organism survival, where in the anoxic stress experiments, lactic acid starts to form as seen with the CH_3 peak labeled in red. (b) Relative change of lactic acid growth over the course of the experiment. Blue dots are the control experiments, and red dots are the anoxic stress conditions. Experiments were taken every 30 min with three *D. magna* in each sample and conducted in triplicate. Error bars represent standard error, however, that the error bars in the control have been doubled to make them easier to visualize. The concentrations are plotted as percent change relative to the first point in both graphs. (c) Workflow of the "exposure" on *D. magna*, on the left, the blue droplet represents the control conditions, and on the right, the red symbol represents the anoxic stress conditions.

anerobic stress response. As a result, lactic acid concentration was seen to increase by ∼250% relative to the control organisms. As in humans, this is a response of bypassing the Krebs cycle and breaking down glucose into lactic acid to produce energy; adenosine triphosphate (ATP).[56] The response in *D. magna* has also been measured in other studies as a stress response indicator.[14,57] The results of the current study can be seen in Figure 4 below. After the experiment, the organisms used as the control (with DMF support) are still alive and able to recover, while the non-DMF organisms are showing early signs of hypoxia (slightly red in color) and are slow moving. One interesting observation is that in the organisms without DMF replenishing their water, the lineshape is slightly broader. This is likely due to slight evaporation (note the plates are not sealed to allow oxygen exchange) or slight migration of the water downward (under the influence of gravity) when not held in place with the DMF electrode activation. This is turn leads to the degradation of the shims. Although to the eye, the well remains full.

Previously, DMF has been used to grow algae cultures,[58] as a bioassay,[31] and to transport living zebrafish embryos without impacting normal hatching rates,[55] but to the authors knowledge, this is the first time it has been utilized to maintain organisms in vivo for subsequent NMR experiments. Additionally, this is the first dual-tuned (^{1}H/^{13}C) NMR example of DMF-NMR.

Challenges, Solutions, and Future Directions. Using this study as a proof-of-concept, it has been shown that organisms can be kept alive in an NMR without exhibiting anoxic stress responses using a vertically oriented DMF device for the first time. This is a critical step as it demonstrates that DMF holds potential as an automated exposure platform where the ability to mix and expose many contaminants under computer control will be paramount. However, several drawbacks and solutions warrant discussion, with the vast majority stemming from the lack of space inside a standard bore NMR system.

The space inside current high-field NMRs is extremely limited, which in-turn limits both the size and amount of DMF electrodes that can be used, impacting the number of different contaminants, nutrients, and water reservoirs housed on a single chip. Here, using the additional 4 μL droplets, it was possible to maintain three organisms for 2 h. However, standard toxicity tests are commonly performed over 48 h, so additional improvements are needed.[1] The limited size of the reservoirs was the major limiting factor here. One improvement could be to lower the temperature, which decreases oxygen consumption by slowing metabolic rate.[15] Unfortunately, the temperate control in the prototype probe used here had to be removed to make room for the microcoil platform. However, as cooling from 21 °C to 5 °C only increases survivability by a factor of 2, while useful, it is not a complete solution. The simplest solution is to increase the size of the reservoirs. The reservoirs on the current chip are already large in width and length (6.6 × 16 mm); however, the droplets are only able to have a height of 0.2 mm (distance between the top and bottom plate). This is the maximum height that can be used in a vertical DMF design as larger gaps cause the droplets to move under gravity even when continual actuation (a constant voltage to keep the droplets from falling) is applied.[36] Meaning that even if a large-bore vertical magnet (i.e., 89 mm) could be used, the maximum droplet volume and size of the array would still be limited. Conversely, in horizontal DMF devices, droplets can be unrestricted in height, with single-sided devices not even having a top plate.[28] In turn, this explains why so much effort was placed on trying to design horizontal coils here, which could have potentially permitted large droplets and 3D DMF devices (droplets stored in

https://doi.org/10.1021/acs.analchem.2c04201
Anal. Chem. 2023, 95, 5858−5866

horizontal layers)[59,60] to provide the space for arrays of contaminants and large reservoirs. Ultimately, when all things are considered, a vertical DMF design in a vertical bore NMR is limited in terms of droplet/reservoir size, need for continual actuation, space for a wide range of contaminants, restricted electrode space, and wire bundles, that a horizontal magnet design would be recommended for future development.

In a horizontal magnet (such as small MRIs, a converted FT-ICR magnet, and some benchtop NMRs), the B_0 field is also horizontal,[61] meaning that the stripline used for DMF here would also be optimal and could be used as is. Even a modest 10−20 cm bore would be enough to house DMF arrays with 100's of electrodes and significant reservoirs. With large, oxygen saturated reservoirs, the devices could be completely sealed, eliminating outside contamination and evaporation. Ultimately, this study demonstrated that it was possible to maintain organisms inside an NMR using DMF technology and developed coil designs that would translate into a horizontal magnet. This provides the foundation for future development in horizontal magnets to develop uncompromised systems that have the potential to control and automate growth and contaminant exposure with few limitations.

CONCLUSIONS

This study outlines the preliminary steps toward automated DMF-NMR of living organisms and has shown that sensitive microcoils coupled with fabricated DMF chips can be used to keep organisms alive inside of an NMR. While much work remains, this method holds immense potential as once perfected, culturing and exposure could be performed under automation. The low biomass requirements and low sample volumes make DMF-NMR integration amenable to studies where only small amounts of media are available for testing, for example, chromatographic isolates from the environment, air particles, or expensive contaminant standards. An example of the latter is microcystins (the toxins produced by algal blooms that contaminate drinking water), which can cost up to $100,000 per mg for some pure standards (prices from Sigma-Aldrich). Other possibilities could be optimization of culturing conditions or using NMR feedback to measure biomass quality and quantity under various nutrient loads. Ultimately, the ability to automate the control of contaminants and conditions of living organisms with in vivo NMR detection is a step toward the next generation of bioanalytical platforms. Future work should consider a horizontal magnet design that would eliminate the vast majority, if not all, the drawbacks identified here in a vertical DMF-NMR design.

ASSOCIATED CONTENT

Supporting Information

The Supporting Information is available free of charge at https://pubs.acs.org/doi/10.1021/acs.analchem.2c04201.

Further methods, horizontal microcoil results/discussion, and *D. magna* metabolite identities (PDF)

AUTHOR INFORMATION

Corresponding Authors

Aaron R. Wheeler − *Department of Chemistry, University of Toronto, Toronto, Ontario M5S 3H6, Canada; Donnelly Centre for Cellular and Biomolecular Research, University of Toronto, Toronto, Ontario M5S 3E1, Canada; Institute for Biomedical Engineering, University of Toronto, Toronto, Ontario M5S 3G9, Canada;* orcid.org/0000-0001-5230-7475; Email: aaron.wheeler@utoronto.ca

Andre J. Simpson − *Department of Chemistry, University of Toronto, Toronto, Ontario M5S 3H6, Canada; Environmental NMR Center, University of Toronto Scarborough, Scarborough, Ontario M1C 1A4, Canada;* orcid.org/0000-0002-8247-5450; Email: andre.simpson@utoronto.ca

Authors

Amy Jenne − *Department of Chemistry, University of Toronto, Toronto, Ontario M5S 3H6, Canada; Environmental NMR Center, University of Toronto Scarborough, Scarborough, Ontario M1C 1A4, Canada*

Sebastian von der Ecken − *Department of Chemistry, University of Toronto, Toronto, Ontario M5S 3H6, Canada; Nicoya, Kitchener, Ontario N2G 2K4, Canada*

Vincent Moxley-Paquette − *Environmental NMR Center, University of Toronto Scarborough, Scarborough, Ontario M1C 1A4, Canada*

Ronald Soong − *Environmental NMR Center, University of Toronto Scarborough, Scarborough, Ontario M1C 1A4, Canada;* orcid.org/0000-0002-8223-9028

Ian Swyer − *Department of Chemistry, University of Toronto, Toronto, Ontario M5S 3H6, Canada*

Monica Bastawrous − *Environmental NMR Center, University of Toronto Scarborough, Scarborough, Ontario M1C 1A4, Canada*

Falko Busse − *Bruker BioSpin GmbH, 76275 Ettlingen, Germany*

Wolfgang Bermel − *Bruker BioSpin GmbH, 76275 Ettlingen, Germany*

Daniel Schmidig − *Bruker BioSpin AG, 8117 Fällanden, Switzerland*

Till Kuehn − *Bruker BioSpin AG, 8117 Fällanden, Switzerland*

Rainer Kuemmerle − *Bruker BioSpin AG, 8117 Fällanden, Switzerland*

Danijela Al Adwan-Stojilkovic − *Bruker BioSpin AG, 8117 Fällanden, Switzerland*

Stephan Graf − *Bruker BioSpin AG, 8117 Fällanden, Switzerland*

Thomas Frei − *Bruker BioSpin AG, 8117 Fällanden, Switzerland*

Martine Monette − *Bruker Canada Ltd., Milton, Ontario L9T 6P4, Canada*

Complete contact information is available at: https://pubs.acs.org/10.1021/acs.analchem.2c04201

Author Contributions

A.J. conducted the metabolomic and in vivo experiments, collected, and analyzed the data. S.V.D.E. and I.S. fabricated the DMF bottom plates, and assembled, maintained, and operated the devices. V.M.-P. designed, fabricated, and tested the microcoils. R.S., M.B., W.B., and A.J.S. assisted with data collection and experiment optimization. F.B., D.S., T.K., R.K., D.A.A.-S., S.G., T.F., and M.M. built the custom NMR probe and gradient. A.J., S.V.D.E., A.R.W., and A.J.S. wrote the manuscript.

Notes

The authors declare no competing financial interest.

https://doi.org/10.1021/acs.analchem.2c04201
Anal. Chem. 2023, 95, 5858−5866

■ ACKNOWLEDGMENTS

A.J.S. would like to thank the Natural Sciences and Engineering Research Council of Canada (NSERC) [Alliance (ALLRP 549399), Alliance (ALLRP 555452), and Discovery Programs (RGPIN-2019-04165)], the Canada Foundation for Innovation (CFI), the Ontario Ministry of Research and Innovation (MRI), the Krembil Foundation for providing funding, and the Government of Ontario for an Early Researcher Award. A.R.W. would like to thank the NSERC Discovery Program (RGPIN 2019-04867). A.J. would like to thank R. Cheng, N. Punjabi, and H-.M. Lin who helped with the microcoil soldering.

■ REFERENCES

(1) Krewski, D.; Acosta, D.; Andersen, M.; Anderson, H.; Bailar, J. C.; Boekelheide, K.; Brent, R.; Charnley, G.; Cheung, V. G.; Green, S.; Kelsey, K. T.; Kerkvliet, N. I.; Li, A. A.; McCray, L.; Meyer, O.; Patterson, R. D.; Pennie, W.; Scala, R. A.; Solomon, G. M.; Stephens, M.; Yager, J.; Zeise, L. *J. Toxicol. Environ. Health B Crit. Rev.* **2010**, *13*, 51−138.
(2) Johnson, C. H.; Ivanisevic, J.; Siuzdak, G. *Nat. Rev. Mol. Cell Biol.* **2016**, *17*, 451−459.
(3) Lin, C. Y.; Viant, M. R.; Tjeerdema, R. S. *J. Pestic. Sci.* **2006**, *31*, 245−251.
(4) Vignoli, A.; Ghini, V.; Meoni, G.; Licari, C.; Takis, P. G.; Tenori, L.; Turano, P.; Luchinat, C. *Angew. Chem., Int. Ed.* **2019**, *58*, 968−994.
(5) Nagana Gowda, G. A.; Raftery, D. *Anal. Chem.* **2017**, *89*, 490−510.
(6) Bembenek Bailey, S. A.; Niemuth, J. N.; McClellan-Green, P. D.; Godfrey, M. H.; Harms, C. A.; Stoskopf, M. K. *R. Soc. Open Sci.* **2017**, *4*, No. 171433.
(7) Majumdar, R. D.; Akhter, M.; Fortier-McGill, B.; Soong, R.; Liaghati-Mobarhan, Y.; Simpson, A. J.; Spraul, M.; Schmidt, S.; Heumann, H. *eMagRes.* **2017**, *6*, 133−148.
(8) Viant, M. R.; Walton, J. H.; Tjeerdema, R. S. *Pestic. Biochem. Physiol.* **2001**, *71*, 40−47.
(9) Shulman, R. G.; Rothman, D. L. *Metabolomics by in Vivo NMR*; John Wiley & Sons, 2004.
(10) Bunescu, A.; Garric, J.; Vollat, B.; Canet-Soulas, E.; Graveron-Demilly, D.; Fauvelle, F. *Mol. BioSyst.* **2010**, *6*, 121−125.
(11) Viant, M. R.; Walton, J. H.; TenBrook, P. L.; Tjeerdema, R. S. *Aquat. Toxicol.* **2002**, *57*, 139−151.
(12) Righi, V.; Apidianakis, Y.; Psychogios, N.; Rahme, L. G.; Tompkins, R. G.; Tzika, A. A. *Int. J. Mol. Med.* **2014**, *34*, 327−333.
(13) Soong, R.; Liaghati Mobarhan, Y.; Tabatabaei, M.; Bastawrous, M.; Biswas, R. G.; Simpson, M.; Simpson, A. *Magn. Reson. Chem.* **2020**, *58*, 411−426.
(14) Bastawrous, M.; Tabatabaei-Anaraki, M.; Soong, R.; Bermel, W.; Gundy, M.; Boenisch, H.; Heumann, H.; Simpson, A. J. *Anal. Chim. Acta* **2020**, *1138*, 168−180.
(15) Tabatabaei Anaraki, M.; Dutta Majumdar, R.; Wagner, N.; Soong, R.; Kovacevic, V.; Reiner, E. J.; Bhavsar, S. P.; Ortiz Almirall, X.; Lane, D.; Simpson, M. J.; Heumann, H.; Schmidt, S.; Simpson, A. J. *Anal. Chem.* **2018**, *90*, 7912−7921.
(16) Adema, D. M. M. *Hydrobiologia* **1978**, *59*, 125−134.
(17) Möst, M.; Chiaia-Hernandez, A. C.; Frey, M. P.; Hollender, J.; Spaak, P. *Environ. Toxicol. Chem.* **2015**, *34*, 338−345.
(18) Bastawrous, M.; Gruschke, O.; Soong, R.; Jenne, A.; Gross, D.; Busse, F.; Nashman, B.; Lacerda, A.; Simpson, A. J. *Anal. Chem.* **2022**, *94*, 8523−8532.
(19) Wagner, N. D.; Simpson, A. J.; Simpson, M. J. *Environ. Toxicol. Chem.* **2017**, *36*, 938−946.
(20) Eroglu, S.; Gimi, B.; Roman, B.; Friedman, G.; Magin, R. L. *Concepts Magn. Reson. Part B Magn. Reson. Eng.* **2003**, *17B*, 1−10.
(21) Fugariu, I.; Soong, R.; Lane, D.; Fey, M.; Maas, W.; Vincent, F.; Beck, A.; Schmidig, D.; Treanor, B.; Simpson, A. J. *Analyst* **2017**, *142*, 4812−4824.
(22) Chen, Y.; Mehta, H. S.; Butler, M. C.; Walter, E. D.; Reardon, P. N.; Renslow, R. S.; Mueller, K. T.; Washton, N. M. *Phys. Chem. Chem. Phys.* **2017**, *19*, 28163−28174.
(23) Fratila, R. M.; Velders, A. H. *Annu. Rev. Anal. Chem.* **2011**, *4*, 227−249.
(24) Fugariu, I.; Bermel, W.; Lane, D.; Soong, R.; Simpson, A. J. *Angew. Chem., Int. Ed.* **2017**, *56*, 6324−6328.
(25) Lane, D.; Liaghati Mobarhan, Y.; Soong, R.; Ning, P.; Bermel, W.; Tabatabaei Anaraki, M.; Wu, B.; Heumann, H.; Gundy, M.; Boenisch, H.; Jeong, T. Y.; Kovacevic, V.; Simpson, M. J.; Simpson, A. J. *Anal. Chem.* **2019**, *91*, 15000−15008.
(26) Bart, J.; Kolkman, A. J.; de Vries, A. J. O.; Koch, K.; Nieuwland, P. J.; Janssen, H. J. W. G.; van Bentum, J. P. J. M.; Ampt, K. A. M.; Rutjes, F. P. J. T.; Wijmenga, S. S.; Gardeniers, H. J. G. E.; Kentgens, A. P. M. *J. Am. Chem. Soc.* **2009**, *131*, 5014−5015.
(27) Bakhtina, N. A.; Korvink, J. G. *RSC Adv.* **2014**, *4*, 4691−4709.
(28) Choi, K.; Ng, A. H. C.; Fobel, R.; Wheeler, A. R. *Annu. Rev. Anal. Chem.* **2012**, *5*, 413−440.
(29) Lienemann, J.; Greiner, A.; Korvink, J. G. *IEEE Trans. Comput. Aided Des. Integr. Circuits Syst.* **2006**, *25*, 234−247.
(30) Ng, A. H. C.; Fobel, R.; Fobel, C.; Lamanna, J.; Rackus, D. G.; Summers, A.; Dixon, C.; Dryden, M. D. M.; Lam, C.; Ho, M.; Mufti, N. S.; Lee, V.; Asri, M. A. M.; Sykes, E. A.; Chamberlain, M. D.; Joseph, R.; Ope, M.; Scobie, H. M.; Knipes, A.; Rota, P. A.; Marano, N.; Chege, P. M.; Njuguna, M.; Nzunza, R.; Kisangau, N.; Kiogora, J.; Karuingi, M.; Burton, J. W.; Borus, P.; Lam, E.; Wheeler, A. R. *Sci. Transl. Med.* **2018**, *10*, No. eaar6076.
(31) Dixon, C.; Lamanna, J.; Wheeler, A. R. *Lab Chip* **2020**, *20*, 1845−1855.
(32) Srinivasan, V.; Pamula, V. K.; Fair, R. B. *Lab Chip* **2004**, *4*, 310−315.
(33) Pollack, M. G.; Fair, R. B.; Shenderov, A. D. *Appl. Phys. Lett.* **2000**, *77*, 1725.
(34) Fobel, R.; Fobel, C.; Wheeler, A. R. *Appl. Phys. Lett.* **2013**, *102*, No. 193513.
(35) Swyer, I.; von der Ecken, S.; Wu, B.; Jenne, A.; Soong, R.; Vincent, F.; Schmidig, D.; Frei, T.; Busse, F.; Stronks, H. J.; Simpson, A. J.; Wheeler, A. R. *Lab Chip* **2019**, *19*, 641−653.
(36) Swyer, I.; Soong, R.; Dryden, M. D. M.; Fey, M.; Maas, W. E.; Simpson, A.; Wheeler, A. R.; Ampt, K. A. M.; Rutjes, F. P. J. T.; Wijmenga, S. S.; Gardeniers, H. J. G. E.; Kentgens, A. P. M. *Lab Chip* **2016**, *16*, 4424−4435.
(37) Liess, M.; Henz, S.; Shahid, N. *Environ. Sci. Eur.* **2020**, *32*, 119.
(38) Moxley-Paquette, V.; Lane, D.; Soong, R.; Ning, P.; Bastawrous, M.; Wu, B.; Pedram, M. Z.; Haque Talukder, M. A.; Ghafar-Zadeh, E.; Zverev, D.; Martin, R.; Macpherson, B.; Vargas, M.; Schmidig, D.; Graf, S.; Frei, T.; al Adwan-Stojilkovic, D.; de Castro, P.; Busse, F.; Bermel, W.; Kuehn, T.; Kuemmerle, R.; Fey, M.; Decker, F.; Stronks, H.; Sullan, R. M. A.; Utz, M.; Simpson, A. J. *Anal. Chem.* **2020**, *92*, 15454−15462.
(39) Moxley-Paquette, V.; Wu, B.; Lane, D.; Bastawrous, M.; Ning, P.; Soong, R.; de Castro, P.; Kovacevic, I.; Frei, T.; Stuessi, J.; al Adwan-Stojilkovic, D.; Graf, S.; Vincent, F.; Schmidig, D.; Kuehn, T.; Kuemmerle, R.; Beck, A.; Fey, M.; Bermel, W.; Busse, F.; Gundy, M.; Boenisch, H.; Heumann, H.; Nashman, B.; Dutta Majumdar, R.; Lacerda, A.; Simpson, A. J. *Magn. Reson. Chem.* **2022**, *60*, 386−397.
(40) Ellinger, J. J.; Chylla, R. A.; Ulrich, E. L.; Markley, J. L. Databases and Software for NMR-Based Metabolomics. *Curr. Metabolomics* **2012**, *1* (), DOI: 10.2174/2213235X11301010028.
(41) Wu, B.; von der Ecken, S.; Swyer, I.; Li, C.; Jenne, A.; Vincent, F.; Schmidig, D.; Kuehn, T.; Busse, F.; Stronks, H.; Soong, R.; Wheeler, A. R.; Simpson, A. J. *Angew. Chem., Int. Ed.* **2019**, *58*, 15372−15376.
(42) Massin, C.; Vincent, F.; Homsy, A.; Ehrmann, K.; Boero, G.; Besse, P.-A.; Daridon, A.; Verpoorte, E.; de Rooij, N. F.; Popovic, R. S. *J. Magn. Reson.* **2003**, *164*, 242−255.

https://doi.org/10.1021/acs.analchem.2c04201
Anal. Chem. 2023, 95, 5858−5866

(43) Kentgens, A. P. M.; Bart, J.; van Bentum, P. J. M.; Brinkmann, A.; van Eck, E. R. H.; Gardeniers, J. G. E.; Janssen, J. W. G.; Knijn, P.; Vasa, S.; Verkuijlen, M. H. W. *J. Chem. Phys.* **2008**, *128*, No. 052202.
(44) Butler, M. C.; Mehta, H. S.; Chen, Y.; Reardon, P. N.; Renslow, R. S.; Khbeis, M.; Irish, D.; Mueller, K. T. *Phys. Chem. Chem. Phys.* **2017**, *19*, 14256−14261.
(45) Fratila, R. M.; Gomez, M. V.; Sýkora, S.; Velders, A. H. *Nat. Commun.* **2014**, *5*, 3025.
(46) Ravi, K. C.; Henry, I. D.; Park, G. H. J.; Aghdasi, A.; Raftery, D. *Concepts Magn. Reson. Part B Magn. Reson. Eng.* **2010**, *37B*, 13.
(47) Olson, D. L.; Peck, T. L.; Webb, A. G.; Magin, R. L.; Sweedler, J. V. *Science* **1995**, *270*, 1967−1970.
(48) Finch, G.; Yilmaz, A.; Utz, M. *J. Magn. Reson.* **2016**, *262*, 73−80.
(49) Ryan, H.; Song, S. H.; Zaß, A.; Korvink, J.; Utz, M. *Anal. Chem.* **2012**, *84*, 3696−3702.
(50) Lei, K. M.; Mak, P. I.; Law, M. K.; Martins, R. P. *Analyst* **2014**, *139*, 6204−6213.
(51) Delaglio, F.; Walker, G. S.; Farley, K.; Sharma, R.; Hoch, J.; Arbogast, L.; Brinson, R.; Marino, J. P. *Am. Pharm. Rev.* **2017**, *20*, No. 339681.
(52) Farooq, H.; Courtier-Murias, D.; Soong, R.; Bermel, W.; Kingery, W. M.; Simpson, A. J. *Curr. Org. Chem.* **2013**, *17*, 3013−3031.
(53) Lei, K. M.; Sun, N.; Mak, P. I.; Martins, R. P.; Ham, D. Micro-NMR on CMOS for Biomolecular Sensing. *CMOS Circuits for Biological Sensing and Processing*, 1st ed.; Springer, 2018. 101−132.
(54) Ng, A. H. C.; Li, B. B.; Chamberlain, M. D.; Wheeler, A. R. *Annu. Rev. Biomed. Eng.* **2015**, *17*, 91−112.
(55) Son, S. U.; Garrell, R. L. *Lab Chip* **2009**, *9*, 2398−2401.
(56) Wilding, M.; Coppola, G.; Dale, B.; di Matteo, L. *Reproduction* **2009**, *137*, 619−624.
(57) Soong, R.; Nagato, E.; Sutrisno, A.; Fortier-Mcgill, B.; Akhter, M.; Schmidt, S.; Heumann, H.; Simpson, A. J. *Magn. Reson. Chem.* **2015**, *53*, 774−779.
(58) Shih, S. C. C.; Mufti, N. S.; Chamberlain, M. D.; Kim, J.; Wheeler, A. R. *Energy Environ. Sci.* **2014**, *7*, 2366−2375.
(59) Jun Lee, S.; Lee, S.; Hyoung Kang, K. *Appl. Phys. Lett.* **2012**, *100*, No. 081604.
(60) Hong, J.; Kim, Y. K.; Won, D. J.; Kim, J.; Lee, S. J. *Sci. Rep.* **2015**, *5*, 10685.
(61) Anders, J.; Dreyer, F.; Krüger, D.; Schwartz, I.; Plenio, M. B.; Jelezko, F. *J. Magn. Reson.* **2021**, *322*, No. 106860.

https://doi.org/10.1021/acs.analchem.2c04201
Anal. Chem. 2023, 95, 5858−5866